

Optical phonon scattering and theory of magneto-polarons in a quantum cascade laser in a strong magnetic field

Yu Chen^{1,2}, N. Regnault¹, R. Ferreira¹, Bang-Fen Zhu² and G. Bastard¹

¹Laboratoire Pierre Aigrain, Ecole Normale Supérieure,
CNRS, 24 Rue Lhomond, F-75005 Paris, France

²Department of Physics, Tsinghua University, Beijing 100084, China
(Dated: February 21, 2024)

We report a theoretical study of the carrier relaxation in a quantum cascade laser (QCL) subjected to a strong magnetic field. Both the alloy (GaInAs) disorder effects and the Frohlich interaction are taken into account when the electron energy differences are tuned to the longitudinal optical (LO) phonon energy. In the weak electron-phonon coupling regime, a Fermi's golden rule computation of LO phonon scattering rates shows a very fast non-radiative relaxation channel for the alloy broadened Landau levels (LL's). In the strong electron-phonon coupling regime, we use a magneto-polaron formalism and compute the electron survival probabilities in the upper LL's with including increasing numbers of LO phonon modes for a large number of alloy disorder configurations. Our results predict a nonexponential decay of the upper level population once electrons are injected in this state.

PACS numbers:

I. INTRODUCTION

A quantum cascade laser (QCL) is a semiconductor laser with specially designed cascade quantum structure to realize unipolar carrier transport and intersubband optical transition, and thus to achieve long-wavelength lasing by overcoming the bandgap limit of the material [1]. Since the first observation of the population inversion in a QCL [2], the mid-infrared, far-infrared and even THz QCL's have been realized though few of them operate at room temperature [3]. It has been observed that the performances of the QCL's deteriorate with temperature quickly when the emission wave length gets longer, a signature of an increasingly detrimental thermal activation of non-radiative losses. Therefore it is important to understand and control the non-radiative paths from the upper state of the lasing transition. A magnetic field B applied parallel to the growth axis has been used as an external parameter to monitor the characteristic of a QCL. In particular, it modulates the output power of the laser with an oscillation period proportional to $1/B$. This output is sensitive to both elastic and inelastic scatterings, which introduce non-radiative relaxation channels to carriers in the Landau level (LL) [4, 5, 6, 7, 8, 9]. Thus it is of interest to study theoretically the relaxation mechanisms of the QCL in the presence of a quantizing magnetic field. Calculations of the LO phonon emission rates in these disordered systems have rarely been reported [10, 11, 12]. Yet, in the $\text{Ga}_{0.47}\text{In}_{0.53}\text{As}$ active-region material the alloy effect nearly reaches its maximum value, with broadening of the LL up to several meV's. Therefore, it is worth devoting more efforts to the understanding whether the notion of phonon emission remains meaningful in LL quantized material.

Assuming a LL structure at high magnetic field, the problem could be tackled in two radically different ways. In the weak electron-phonon coupling case, the electron

states are initially computed by including alloy scattering potentials and the phonon emission rates are then calculated using the Fermi's golden rule. This traditional perturbative computation would give an estimate of the exponential decay rate of the upper level electron population. On the contrary, LL electrons and LO phonons form magneto-polaron states when their coupling is strong enough. Similar effects appear recurrently in the optical properties of quantum dots (QD's), e.g.: [13, 14]. In this mixed mode description the electron-LO phonon interaction is initially taken into account exactly. Hence, the very notion of phonon scattering/emission becomes irrelevant. We shall examine the magneto-polaron case where the alloy scattering broadens the magneto-polaron states and compute the time-dependent survival probabilities in the upper LL's for an electron initially in one of the alloy broadened upper LL's. This electron-phonon strong coupling theory leads to a distinguishably different prediction for the carrier relaxation process as compared to the ordinary phonon emission picture, and predicts a nonexponential population decay from the upper levels.

II. LO PHONON EMISSION OF THE ALLOY BROADENED LL'S

For mid-infrared QCL's, it is a reasonable assumption that the alloy scattering destroys neither the subband structure at zero field nor the LL structure at high magnetic fields. So we consider only a few subbands and their LL's. Leuliet et al demonstrated that the alloy scattering effect in the barrier is negligible as compared to that in the well [11]. We correspondingly model the active region of a QCL as a single quantum well (QW) clad between infinite potential barriers along the z direction. A uniform magnetic field applied parallel to the quantum confinement direction is considered in Landau gauge

(with the vector potential $\mathbf{A} = B x \hat{y}$). Moreover, we neglect the spin Zeeman effect. Thus, in the effective mass model the unperturbed degenerate LL eigenstates of the l th subband read

$$\begin{aligned} \psi_{E_1;n;k_y} &= \frac{1}{\sqrt{L_y}} e^{ik_y y} \phi_n(z) \exp(i k_y x); \\ \epsilon_{l,n} &= E_1 + n + \frac{1}{2} \omega_c; \end{aligned} \quad (1)$$

where ϕ_n as the wavefunction of the n th subband, ϕ_n the n th Hermite function, $\ell = \sqrt{\hbar/eB}$ the magnetic length and $\omega_c = eB/\hbar m$ the cyclotron frequency. We take $m = 0.05m_0$ for electron effective mass and $L_z = 12.33\text{nm}$ for quantum well width, which gives the zero-field subband separation $E_2 - E_1 = 147.5\text{meV}$. The LL degeneracy (per spin) is $D = L_x L_y / (2\ell^2)$.

For a numerical calculation of the alloy scattering effect in the $\text{Ga}_{1-x}\text{In}_x\text{As}$ well, we partition the system (a large box of $L_x = L_y = L_z = 99.79\text{nm} \times 99.79\text{nm} \times 12.33\text{nm}$) into tiny unit cells ($\ell_0 = 2.93\text{\AA} \times 2.93\text{\AA} \times 5.87\text{\AA}$) [15]. In each cell the scattering potential is a random variable which equals to xV with probability $1-x$ and to $(1-x)V$ with probability x , where $x = 0.53$ for $\text{Ga}_{0.47}\text{In}_{0.53}\text{As}$ and $V = 0.6\text{eV}$ [16]. On the scale of LL's or z dependent wavefunction extensions, the alloy fluctuations act like delta scatterers and we assume there is no correlation between the x values of different cells. Thus the alloy potential is given by [17]

$$V_{\text{alloy}} = \sum_{\mathbf{R}_{Ga}} x (\psi_{Ga}) - \sum_{\mathbf{R}_{In}} (1-x) (\psi_{In}) : \quad (2)$$

With a given configuration of the alloy disorder, we calculate the alloy broadened LL's by diagonalizing the alloy potential in the basis of the degenerate LL's (for details, see Ref. [15]). With our sample box this means $D = 59$ states per LL at 24.58T . The diagonalization has been done with $N = 100$ samples with randomly distributed alloy atoms.

The numerical results (Figs. 1 and 2) demonstrate the validity of the LL structure and clearly show the localization of the electrons at the broadened LL's tails as well as the extended behavior at the maximum of the density of states (DOS). Fig. 1 shows the in-plane electron density distributions $P(\mathbf{r})$ for four states of one particular alloy configuration, as defined by

$$P_{l,n}(\mathbf{r}) = \int_{-\infty}^{\infty} |\psi_{l,n}(z)|^2 dz \quad (3)$$

where $\psi_{E_1;n} = \phi_n(z) \psi_n(\mathbf{r})$ is the n th disordered state related to $E_1;n$ (a short notation for all unperturbed or disordered states related to the l th subband and n th LL's). For each of the $E_1;n$ states of a par-

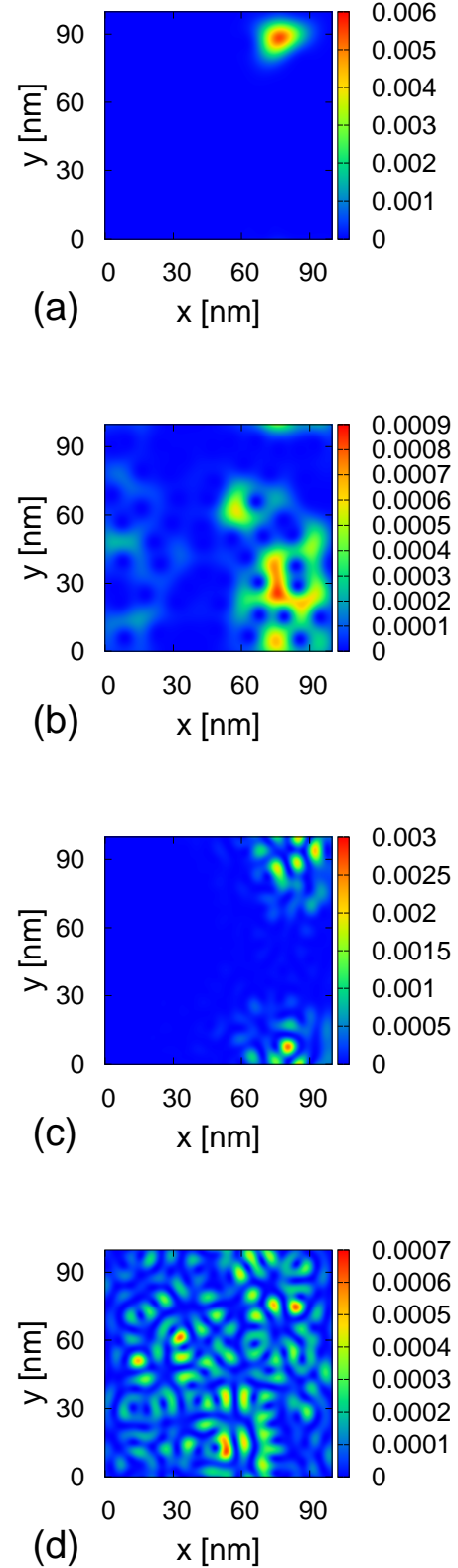


FIG. 1: (Color online) Typical in-plane electron density distributions (in \AA^{-2}) for four states in the set of independently broadened LL's at 24.58T : (a) DOS tail of $|E_2;0\rangle$; (b) DOS max of $|E_2;0\rangle$; (c) DOS tail of $|E_1;2\rangle$; (d) DOS max of $|E_1;2\rangle$.

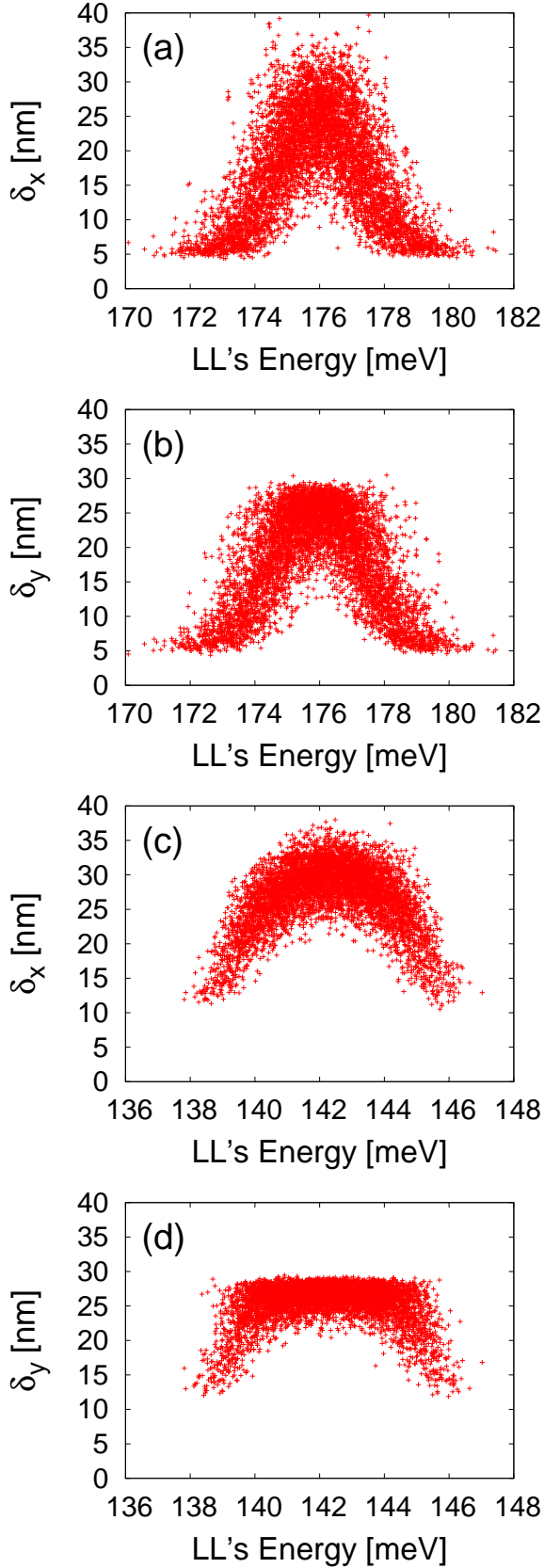


FIG. 2: (Color online) Position uncertainties of the independently alloy broadened LL's at 24.58T: (a) δ_x of $|E_2;0\rangle$; (b) δ_y of $|E_2;0\rangle$; (c) δ_x of $|E_1;2\rangle$; (d) δ_y of $|E_1;2\rangle$.

ticular run, we have computed the x- and y-uncertainties,

$$\delta_x = \frac{q}{\sqrt{\sum x^2}}; \quad (4)$$

$$\delta_y = \frac{q}{\sqrt{\sum y^2}}; \quad (5)$$

Fig. 2 shows δ_x and δ_y for all the independently alloy disordered states related to $E_2;0$ or $E_1;2$ at 24.58T ($D = 59$; $N = 100$ disorder configurations). For an unbroadened LL $E_1;n;k_y$ with the electron entirely delocalized along the y axis over a segment L there is $\delta_y = \frac{L}{2\sqrt{3}}$ and $\delta_x^{(n)} = \frac{1}{n + \frac{1}{2}}$. For $L = 10^2 \text{ nm}$ and $B = 24.58 \text{ T}$, this means $\delta_y = 28.3 \text{ nm}$, $\delta_x^{(0)} = 3.66 \text{ nm}$ and $\delta_x^{(2)} = 8.18 \text{ nm}$. Fig. 2 shows that the tail states are considerably more localized than the central states. Indeed, for the latter δ_y is close to the expected value for a plane wave. We also note that $\delta_x^{(0)}$ and $\delta_x^{(2)}$ are considerably larger than 3.66 nm and 8.18 nm, respectively, and in fact close to δ_y . This proves that the extended states of the alloy broadened LL's are very different from the unperturbed $E_1;n;k_y$ states but display similar extensions along the x and y directions (the small discrepancies are due to the different boundary conditions along the x and y directions).

We consider the electron-phonon interaction here only due to the GaAs-like LO phonons, because in the $\text{Ga}_{0.47}\text{In}_{0.53}\text{As}$ alloy the Frohlich interaction is dominant and the potential of GaAs-like modes dominates over that of the InAs-like modes [18]. We take the zone-center LO mode frequency as $\omega_{LO} = 33.7 \text{ meV}$ and the Frohlich interaction as

$$H_{e-ph} = \sum_{\mathbf{q}} \frac{g}{q} e^{i\mathbf{q} \cdot \mathbf{r}} b_{\mathbf{q}}^{\dagger} + \text{h.c.} \quad (6)$$

where $b_{\mathbf{q}}^{\dagger}$ is the creation operator of an LO phonon with a wavevector of \mathbf{q} and the Frohlich factor is $g = \frac{e^2 \omega_{LO}}{2\pi_0 V_{cr}} (\frac{1}{\epsilon_1} - \frac{1}{\epsilon_s})$ with $\epsilon_1 = 11.6$ and $\epsilon_s = 13.3$ as the high-frequency and static relative dielectric constants of GaAs material, respectively, and V_{cr} the crystal volume.

In the absence of the alloy-disorder, the unperturbed factorized states $E_2;n_2=0;k_y=0_{LO}$ and $E_1;n_1=p \neq 0;k_y=1_{LO}$ cross at the edge $B_p = m(E_2 - E_1 - \omega_{LO}) = (p-1)\omega_{LO}$ for any values of k_y and k_y^0 . Let us consider the $p=2$ resonance, for which the turn on of QCL's lasing has been numerically calculated under the assumption of a dominant inhomogeneous broadening [11]. We can calculate the scattering rate due to the electron-phonon interaction from one of the alloy broadened $E_2;0$ LL states towards any of the $E_1;2$ broadened states assuming the Fermi's golden rule holds. The scattering frequencies are averaged over different alloy configurations. As shown in Fig. 3, at resonance ($B_2 = 24.58 \text{ T}$) the scattering rate of this irreversible departure from the initial state reaches a maxi-

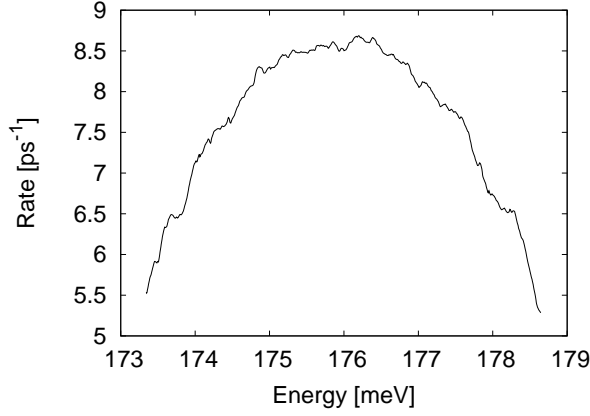


FIG. 3: LO phonon emission rate from alloy broadened LL's $|E_2;0\rangle$ to alloy broadened LL's $|E_1;2\rangle$ at $B_2 = 24.58\text{T}$, as a function of the energy of the initial state.

maximum value when the initial state coincides with the center of the broadened LL's; this energy also corresponds to the largest DOS of the initial states. Note that in spite of the fact that we deal with transitions between different LL's associated with different subbands, the scattering rate is quite large: we find in Fig. 3 a maximum scattering rate of 8.66ps^{-1} . This relatively large value results from the increased DOS of initial states due to the Landau quantization even in the presence of disorder. It also points out a difficulty in applying blindly the Fermi's golden rule since the energy uncertainty $\sim 5.70\text{meV}$ due to LO phonon emission is comparable to the LL width due to alloy broadening (with the full width at 1/e DOS max as 5.69meV , see Ref. [15] and also Sec. III).

III. ALLOY BROADENED MAGNETO-POLARON STATES AND THE SURVIVAL PROBABILITY IN THE UPPER LL'S

A. Unperturbed magneto-polaron states

As shown in the Fig. 4, the Frohlich interaction replaces the crossing of $E_2;0$ 0_{LO} and $E_1;p$ 1_{LO} by an anticrossing and leads to the formation of mixed magneto-polaron states. These are obtained by diagonalizing the Frohlich interaction in the factorized states manifold [19], and read:

$$\begin{aligned}
 |p; k_y\rangle &= \sum_{\mathbf{q}} \left(\langle p; E_2; 0; k_y | 0 \rangle + \langle p; E_1; p; k_y | \mathbf{q} \rangle \right) |1_{\mathbf{q}}\rangle; \\
 |p\rangle &= \frac{1}{1 + \frac{2}{\mathbf{q}^2}}; \quad \langle p; \mathbf{q} | = \frac{i g_p}{\mathbf{q}^2} \langle p | I_p(\mathbf{q}); \\
 |p\rangle &= |2; 0\rangle + \frac{1}{2} |p\rangle; \quad |p\rangle = \frac{p}{2} \frac{p}{4} + \frac{2}{p}; \quad (7)
 \end{aligned}$$

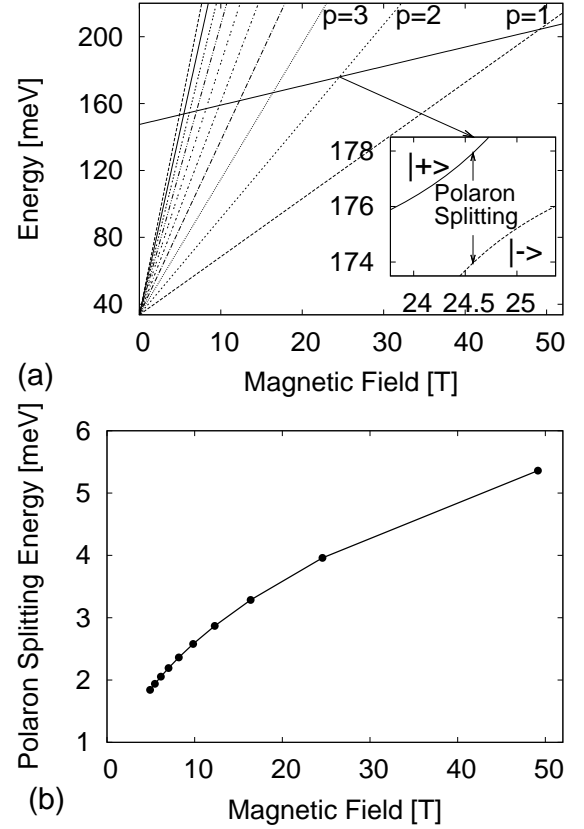


FIG. 4: Illustrations of magneto-polaron states in ideal systems. (a) A schematic picture of the formation of magneto-polaron states. Insert: energy anticrossing around $B_2 = 24.58\text{T}$. (b) Polaron splitting energies as a function of B_p for $p = 1$ to 10 (the line is only a guide for the eyes).

where \pm refers to the upper (+) and lower (−) polaron states in Figure 4(a), the detuning energy is $\sim_p = \langle 1_p | + \langle 1_{LO} | 2; 0 \rangle$, and the half polaron splitting energy is given by

$$\sim_p = \frac{S}{\mathbf{q}} \frac{\mathbf{q}^2}{g_p^2} \langle \mathbf{q} | \mathbf{q}^2; \quad (8)$$

with the electron-phonon interaction coupling matrix element as

$$\begin{aligned}
 I_p(\mathbf{q}) &= \langle E_2; 0; k_y | e^{i\mathbf{q} \cdot \mathbf{r}} | E_1; p; k_y | \mathbf{q} \rangle \\
 &= \frac{(i\mathbf{q} \cdot \mathbf{q}_y)^p}{p!} \exp\left(-\frac{\mathbf{q}^2}{4}\right) i^2 \mathbf{q}_x \cdot \mathbf{q}_y \frac{\mathbf{q}_y}{2} \\
 &\quad \int dz_2(z) e^{i\mathbf{q}_x \cdot \mathbf{z}} \psi_1(z); \quad (9)
 \end{aligned}$$

Actually, after the diagonalization, we find several uncoupled $E_1; p$ LL's one-phonon replica states in addition to the magneto-polaron states. These uncoupled states cannot be populated by electrons entering the active region directly from the zero-phonon states of the injection region. For simplification, in this section we

concentrate on the magneto-polaron states only (the role of uncoupled states is discussed in Sec. IV). The electron-phonon scattering obeys the momentum conservation law. Since each of the unperturbed LL's has a definite k_y , the Frohlich interaction conserves the k_y number and, consequently, each magneto-polaron state has a definite k_y value in the ideal system. For the case of the exact resonance between $E_2; 0 \rightarrow 0_{LO}$ and $E_1; p \rightarrow 1_{LO}$ the upper and lower polaron branches $p; k_y$ have equal weights of phonon components while for a finite energy detuning these weights are unequal. This is similar to the case of strong coupling between atoms and photons in cavity QED except that each polaron branch has a degeneracy of the LL's [20]. The polaron splitting energy has a B dependence and is about 40 meV at $B_2 = 24.58T$ [19].

B. Disordered polaron DOS: SCBA and numerical results

The alloy disorder breaks the k_y -related translational invariance and thus either broadens the magneto-polaron states (weak disorder) or even destroys the polaron picture (strong disorder). As for quantitative estimate, by using the self-consistent Born approximation (SCBA) [21], we solve a pair of coupled equations of the self-energy of polarons given by

$$\Sigma_{+p}^{(n)} = \frac{\overline{V_{+p;p}^2}}{n_{+p} - \Sigma_{+p}^{(n)}} + \frac{\overline{V_{+p;p}^2}}{n_p - \Sigma_p^{(n)}}; \quad (10)$$

$$\Sigma_p^{(n)} = \frac{\overline{V_{+p;p}^2}}{n_{+p} - \Sigma_{+p}^{(n)}} + \frac{\overline{V_{p;p}^2}}{n_p - \Sigma_p^{(n)}}; \quad (11)$$

where the alloy squared scattering matrix element is averaged over the alloy fluctuations [15], viz.

$$\overline{V_{a;b}^2} = \frac{D}{k_y^0} \sum_{k_y} a; k_y V_{alloy} b; k_y^0 \quad (12)$$

For infinitely large (2-dimensional) samples we have

$$\overline{V_{p;p}^2} = \frac{D}{0} \left[\frac{\frac{3}{2} + \frac{W_p}{\sim^2 \Gamma_p^2} + \frac{U_p}{\sim^4 \Gamma_p^4}}{1 + \frac{2}{p} \frac{1}{\Gamma_p^2}} \right] V_x^2; \quad (13)$$

$$\overline{V_{+p;p}^2} = \frac{D}{0} \left[\frac{\frac{3}{2} + \frac{W_p}{\sim^2 \Gamma_{+p}^2} + \frac{U_p}{\sim^4 \Gamma_{+p}^4}}{1 + \frac{2}{p} \frac{1}{\Gamma_{+p}^2}} \right] V_x^2; \quad (14)$$

where $V_x^2 = x(1-x)V^2$ and each of the alloy squared scattering matrix elements involves two alloy scattering events and consequently contains three terms: zero-phonon term when both events occur among zero-phonon states; one-phonon term when one event occurs among

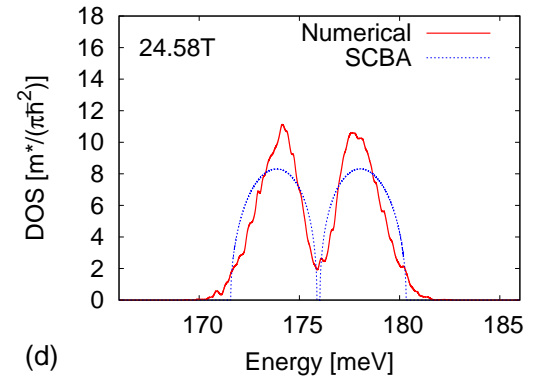
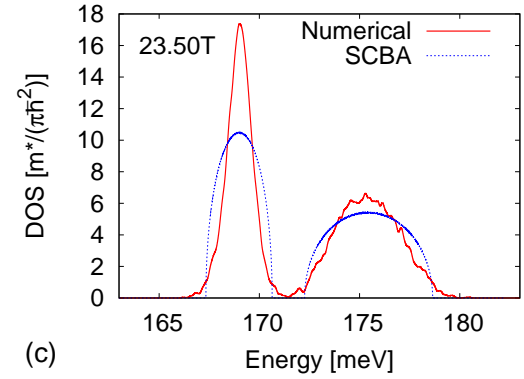
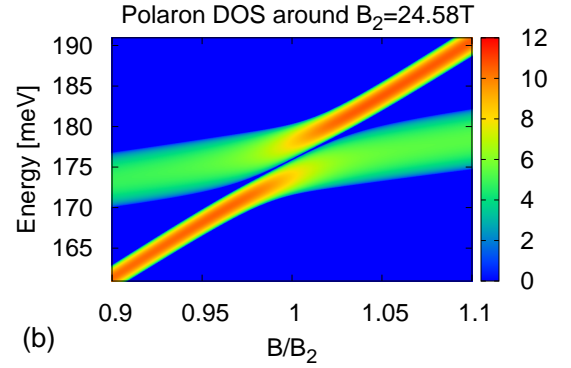
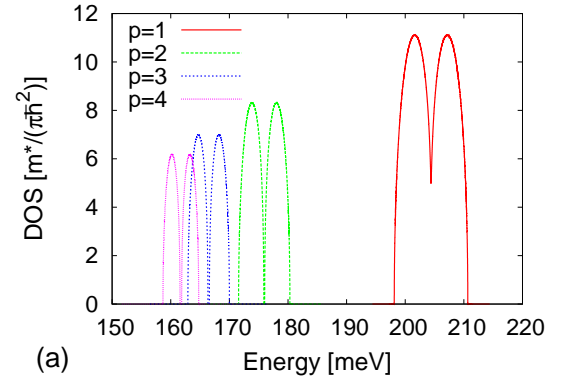


FIG. 5: (Color online) Alloy disorder broadening of magneto-polarons: (a) SCBA calculation of the polaron DOS for $p = 1$ to 4 at the resonant fields B_p ; (b) SCBA calculation of the polaron DOS (in unit of $m^*/(\pi\hbar^2)$) around $B_2 = 24.58T$; (c) and (d) are numerical results at 23.50T and 24.58T, respectively, to compare with the SCBA calculations.

zero-phonon states and the other among one-phonon states; two-phonon term when both events occur among one-phonon states. The one-phonon term has a common factor as

$$W_p = \frac{g^2}{2^{p-1}p!} \sum_{\mathbf{q}=(\mathbf{q}_-, \mathbf{q}_+)} \frac{I_p(\mathbf{q})^2}{q^2} q_-^{2p} \exp\left(-\frac{1}{2} q_-^2\right); \quad (15)$$

and the two-phonon term's factor reads

$$U_p = \frac{3g^4}{2} \sum_{\mathbf{q}\mathbf{q}^0} \frac{I_p(\mathbf{q})I_p(\mathbf{q}^0)}{q q^0} \sum_{k=0}^p \frac{p!}{(p-k)!(k!)^2 2^k} q_-^{2k} q_+^{2(p-k)} \exp\left(-\frac{1}{2} q_-^2\right); \quad (16)$$

Once the magneto-polaron self energy is obtained by iteration, the polaron DOS near B_p is given by

$$\rho'' = \frac{D}{\pi} \text{Im} \left[\frac{1}{\epsilon''_{+p} + \epsilon''_p} + \frac{1}{\epsilon''_{-p} + \epsilon''_p} \right]; \quad (17)$$

As shown in Fig. 5(a), the alloy broadening effect is enhanced with increasing magnetic field. For larger p the alloy broadening may be smaller than the polaron splitting. However, when p is large enough B_p is very close to B_{p+1} so that the two-LL's formalism [Eqs. (10) and (11)] is no longer valid. To set a criterion, we find that a finite polaron gap will open when $\frac{2V_{+p;p}^2}{\sqrt{V_{+p;p}^2 + V_{+p;-p}^2}} < \sim p$. We

can see from Fig. 5(a) that this criterion is not fulfilled for $p=1$ and only marginally for $p=2$, but holds for larger p values with recognizable double maxima in the DOS. In Fig. 5(b-d) we show more results for the SCBA polaron DOS of $p=2$.

We have also performed a numerical diagonalization of the alloy Hamiltonian for a given realization of disorder within a basis of polaron $|k_y\rangle$ states. Once the polaron levels are calculated the density of states is calculated and an average over $N=100$ samples is performed. As seen in Figs. 5(c) and 5(d), the numerical calculations agree quite well with the SCBA results though the broadening effects appear larger in the numerical outputs. We can see in both SCBA and numerical calculations that out of resonance (Fig. 5(c)) the DOS displays two peaks of uneven heights.

The DOS peaks of the two broadened LL's appear very asymmetrical at large detunings. The polaron level that resembles the $E_2;0$ 0_{L0} LL (far from resonance) acquires a width and a shape that goes smoothly to those of the pure electron $E_2;0$ LL [15]. On the other hand, at large detuning the SCBA broadening becomes insufficient to fully account for the alloy broadening. This is because a large number of uncoupled states become nearly degenerate with the polaron levels that resemble the one-LO-phonon replica states $E_1;p=1$ 1_{L0} and these uncoupled states are not accounted for neither in the SCBA

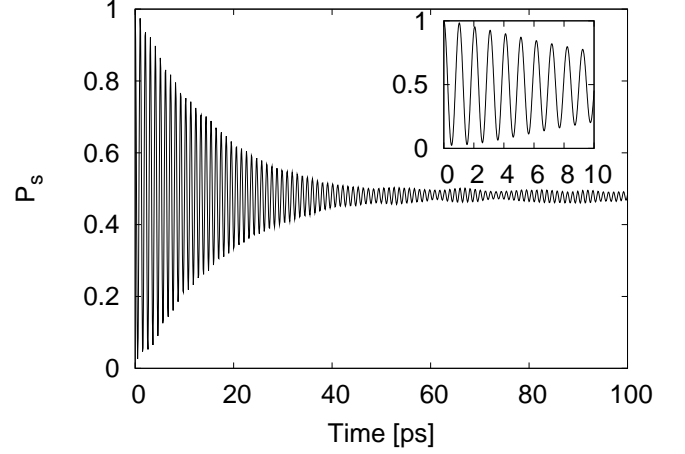


FIG. 6: Survival probability P_s for $B_2 = 24.58T$ with the initial state as the central level of the broadened $|E_2;0\rangle$ LL's while neglecting all the uncoupled states.

equations nor in the numerical results in Fig. 5 (see Sec. IV).

C. Time-dependent survival probability in the upper LL's

The irreversible emission of LO phonon is the most efficient energy relaxation mechanism in QCL at zero magnetic field provided it is energy allowed. In the presence of a strong field, in an ideal sample, this irreversible emission is impossible because of the formation of intersubband magneto-polarons. Alloy scattering blurs the magneto-polaron states and it is interesting to ascertain the nature of the phonon emission in QCL subjected to a strong quantizing magnetic field. To this end, in the case of the $p=2$ resonance, we compute for a given realization of the alloy disorder the survival probability in the ensemble of independently broadened LL states related to $E_2;0$ once the carrier has been injected in one particular state 0_0 of this ensemble:

$$P_s(t) = \sum_{\mathbf{0}} | \langle 0_{L0} | \exp\left(-\frac{iHt}{\hbar}\right) | 0_0 \rangle |^2; \quad (18)$$

where $H = H_e + V_{\text{alloy}} + H_{\text{ph}} + H_{\text{eph}}$. In the following, we take 0_0 as the central level of the broadened ensemble. Once this is achieved we average over the $N=100$ realizations of the alloy disorder. Several magnetic fields have been considered.

When there is a large energy detuning between the zero-LO-phonon replica of $E_2;0$ LL's and the one-LO-phonon replica of $E_1;p=2$ LL's, the survival probability very quickly oscillates between 1 ($t=0$) and P_{min} to stabilize to $P_1 = (1 + P_{\text{min}})/2$ in a characteristic time of a few picoseconds: if 0_0 is the central state of the broadened LL's and for $B=20T$, we find $P_{\text{min}} \approx 0.2$ ps and

$P_1 = 0.83$. Right at resonance $B_2 = 24.58T$, see Fig. 6, the averaged survival probability displays a large number of fast oscillations (pseudo period: 1.03ps) with a decaying amplitude (42ps) that brings P_s to the limiting value $P_1 = 1/2$. We note that the pseudo period is close to $\tau_2 = 1.04ps$. The limiting value $1/2$ recalls the fact that the Frohlich interaction being so efficient that the carrier very quickly exits from the initial state. However, once in the one-LO-phonon replica of the $p = 2$ LL, there is no sink mechanism the electron can use to escape from this LL. Thus, another Frohlich interaction brings it back into the $E_2;0$ LL. There is no reason a priori for this state to be the same as the initial state. Subsequently, the electron leaves the initial LL and oscillates back and forth between the zero-LO-phonon replica of $E_2;0$ LL's and the one-LO-phonon replica of $E_1;p = 2$ LL's. This oscillatory cycle between the two broadened LL's is however irreversible to the extent that the initial state has very little chance to be recovered after $2j$ jumps. This is in striking contrast with the coherent polaron oscillations that would result if there were no alloy scattering acting to blur the polaron states, thereby leading to an oscillatory cycle between only two polaron states.

The consequence on our understanding of the experimentally observed QCL oscillatory output versus B is significant. Unless one can find a plausible and fast escape mechanism from the one-LO-phonon replica, there is no reason to invoke an irreversible escape from the upper state of the lasing transition in a QCL. The long lived oscillations displayed in Fig. 6 will actually be limited by the finite lifetime of the phonons due to anharmonicity effects. This lifetime is about 10ps at low temperature and a few picoseconds at room temperature in bulk GaAs. Similar values were found in InAs self organized QD's [22]. Beyond this lifetime, on average, the oscillations should stop and the electron should have relaxed to one of the disorder broadened LL states $E_1;p$ with no phonon. Note that such a relaxation path would be in complete contrast with bulk and QW materials at zero magnetic field but much in agreement with the energy relaxation scenario established in QD's [14].

IV. EFFECTS OF THE UNCOUPLED ONE-PHONON STATES IN THE STRONG COUPLING REGIME

The approximation of neglecting the uncoupled one-phonon states turns out unsatisfactory because of the very efficient alloy scattering between magneto-polarons and uncoupled one-phonon states. As a result, the Rabi oscillations due to polaron effects will be severely damped since the alloy scattering between polaron states and the large number of uncoupled one-phonon states will give fast additional leakage channels for the LL electrons. The uncoupled states related to the $p; k_y$ polaron are ap-

proximately

$$\begin{aligned} \text{uncoupled} &= E_1;p;k_y - \epsilon_y - 1_{\epsilon};k_y \notin k_y; \\ \text{"uncoupled} &= \text{"}_{1p} + \sim \text{"}_{LO} : \end{aligned} \quad (19)$$

There are $N_{\text{uncoupled}} = (D+1)N_{\text{phonon}}$ such uncoupled states for each pair of $p;k_y$ (where $N_{\text{phonon}} = 480$ discretized LO phonon modes should be included to reproduce accurately the polaron gap, and an accurate numerical diagonalization would give the number in total as $N_{\text{uncoupled}} = (D+1)(N_{\text{phonon}} + 1)$). Note also that these states are energetically placed between the two polaron levels $p;k_y$: at their mid-distance at resonance $B = B_p$ and tend towards the fast increasing (with field) polaron branch at high detuning $B \gg B_p$.

The effect of alloy disorder is twofold: (i) broadening the uncoupled level and (ii) admixing the uncoupled with the polaron states. However, a full diagonalization, including all polaron and uncoupled one-phonon states with a large number of phonon modes, is too heavy numerically (this would mean diagonalizing for each run of the $N = 100$ a matrix of the size as $\text{Dim}(H) = (D+1)(N_{\text{phonon}} + 1)^2 \approx (2.8 \cdot 10^4)^2$). In the following, we present estimates illustrating the importance of effects (i) and (ii).

An estimate of the effect is obtained by remarking that at the lowest order in V_{alloy} it produces a shift of the polaron states which reads

$$S_p = \frac{P_{\text{uncoupled}} + p V_{\text{alloy}} \text{uncoupled}^2}{\text{"}_p \text{"uncoupled}} : \quad (20)$$

It is difficult to give a simplified analytical expression of s_p like Eqs. (13-14) due to the large value of N_{phonon} required. With the results of the numerical diagonalization as shown in Fig. 5(d), this shift is roughly 0.4meV at resonance $B = B_2$, and the effect (ii) becomes very important at increasing detuning $\sim \tau_2$ to the polaron branch whose $\text{"}_{\text{polaron}}$ tends towards $\text{"}_{\text{uncoupled}}$. For increasing $\sim \tau_2$ it becomes necessary to take into account higher orders' effects of V_{alloy} , once the uncoupled one-phonon states enter the DOS of the closer broadened polaron branch. Thus it turns out to be extremely inefficient to handle the problem by making corrections to the SCBA Eqs. (10-11).

Another way to evidence the importance of the coupling between the polaron and the unadmixed states consists in looking at the irreversible escape from one of the polaron states to the unadmixed states broadened by alloy scattering. An estimate using Fermi's golden rule gives at resonance $B = B_p$

$$\begin{aligned} \frac{\sim}{2} \text{"}_p &= \sum_{p;\epsilon} \sum_{\epsilon;k_y^0} E_1;p;k_y - \epsilon_y - V_{\text{alloy}} E_1;p;k_y^0 \\ &\quad \text{"}_p \text{"}_p ; \end{aligned} \quad (21)$$

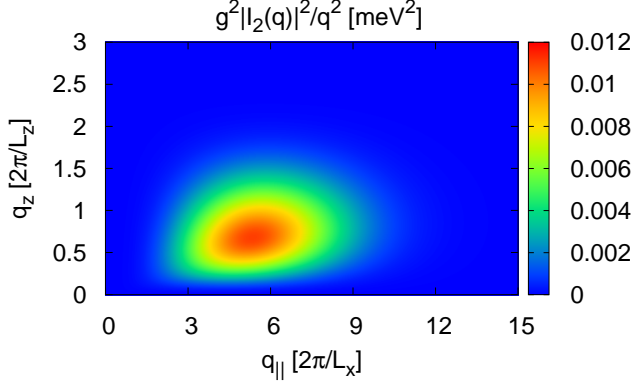


FIG. 7: (Color online) Electron-LO-phonon coupling element related to Frohlich factor versus phonon wave vector.

where the DOS for one of the unadmixed states is written

$$g^2 = \frac{L_x L_y}{2^2 2V_{lp,lp}^2} \frac{V_{lp,lp}^2}{2} \frac{g_{uncoupled}^2}{2} : (22)$$

Putting numbers we find $\tau \approx 0.8$ ps, i.e. comparable to the polaron period. Thus, it is invalid to neglect the uncoupled one-phonon states and effect (ii) is strong enough to generate states without well-defined polaronic character. Note that this result is peculiar to the alloy scattering we have used for static scatterers. In GaAs based QCL's the alloy scattering is negligible and the interface defects are definitely weaker scatterers [10, 11]. Hence, for those materials the polaron levels should be significantly more long-lived.

Therefore, we have included the uncoupled states in the numerical computation of the electron time-dependent survival probability in the upper LL's $E_2;0$ (Eq. (18)). We take a certain number of phonon modes and ensure that the half polaron splitting energy $\sim 2 \times 1.8$ meV since a small portion of the phonons give dominant contributions to the electron-phonon coupling (Fig. 7). As an approximation, we choose a smaller quantization size in the quantum well free dimension (viz. $L_x \times L_y \times L_z$) for the phonon modes than for the LL's electrons (which is $L_x \times L_y \times L_z$). In the z-dimension, a specified wavevector is chosen for the phonon modes (typically $2\pi/L_z$). Numerical computations of the upper LL's survival probabilities with initially putting an electron in the center of the LL's $E_2;0$ have been done with $N_{\text{phonon}} = 20$, $\Delta E_{\text{ph}} = (1.2 \times 10^3)^2$, $N_{\text{phonon}} = 36$, $\Delta E_{\text{ph}} = (2.2 \times 10^3)^2$, $N_{\text{phonon}} = 56$, $\Delta E_{\text{ph}} = (3.4 \times 10^3)^2$ and $N_{\text{phonon}} = 88$, $\Delta E_{\text{ph}} = (5.3 \times 10^3)^2$ (Fig. 8(a)) for $B_2 = 24.58$ T (for $N_{\text{phonon}} = 1$ more than 384 modes are required). We see that at resonance (Fig. 8(a)) the survival probability in the $E_2;0$ LL's decays very rapidly with time: in about 0.6 ps it has dropped to nearly zero. The decay is almost insensitive to the number of uncoupled phonon

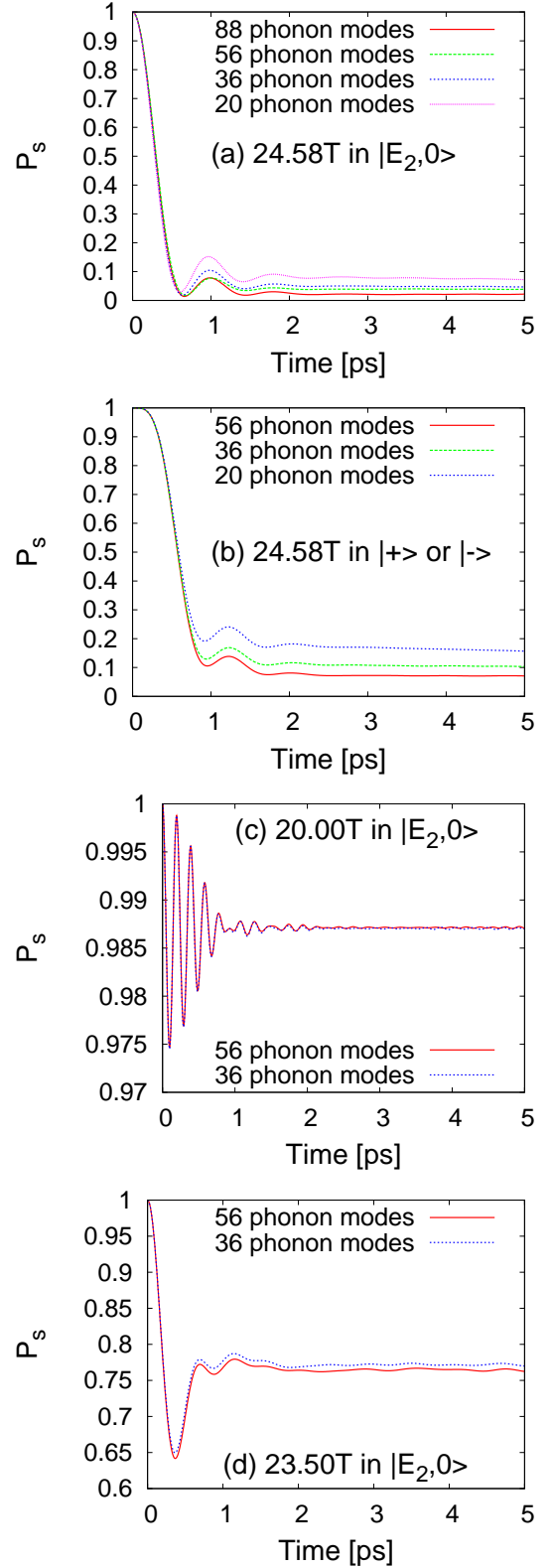


FIG. 8: (Color online) Taking increasing numbers of the uncoupled one-phonon states into account, computations of the electron survival probabilities with initial state in center of the alloy broadened LL's $|E_2;0\rangle$: (a) remaining in $|E_2;0\rangle$ at $B_2 = 24.58$ T; (b) in polaron states $|+\rangle$ or $|-\rangle$ at B_2 ; (c) in $|E_2;0\rangle$ at 20.00 T; (d) in $|E_2;0\rangle$ at 23.50 T (see text).

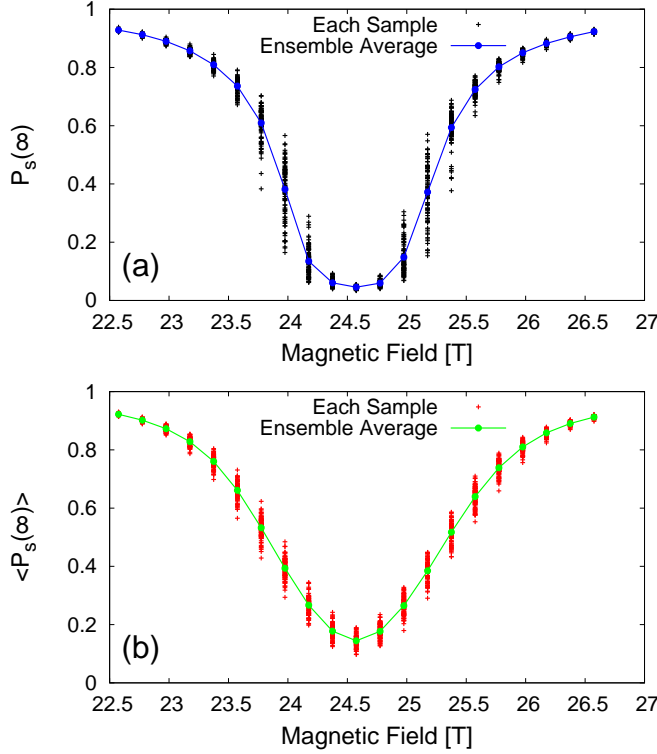


FIG. 9: (Color online) Computations with 36 phonon modes of the long time limit of the survival probability $P_s(1)$ in the $|E_2;0\rangle$ LL's: (a) Initial states in center of LL's $|E_2;0\rangle |0_{LO}\rangle$ for each sample; (b) Average over all initial LL's $|E_2;0\rangle |0_{LO}\rangle$ for each sample. Also the ensemble averages are taken over the $N=100$ samples for each case (joined by lines, which are guides for the eyes).

modes and in fact coincides with the one shown in Fig. 6. However, instead of recovering to $1/2$ at long time, P_s remains very small and displays faint remnants of the polaron oscillations. This is the irreversible oscillation between the polaron branches and the $N_{\text{uncoupled}}$ uncoupled phonon modes that explains the lack of recovering after the first oscillation.

In Fig. 8(b) we show the survival probability of remaining in the polaron states with the same initial state as that of Fig. 8(a). It should be noticed that at the first half picosecond the polaron effect is still strong enough to hold its pseudo oscillation against the damping due to the alloy scattering effect. The same calculation of the probabilities in $E_2;0$ for lower magnetic fields near B_2 are shown in Figs. 8(c) and 8(d). The Figs. reveal that, out of the resonant field and in the presence of both alloy and LO phonon scatterings, the probability of relaxing to the lower LL's remains small at long time.

The experimental implication of our findings on the resonant non-radiative relaxation in the QCL's subjected to a quantizing magnetic field can be illustrated in the following way. For one realization of disorder and a given magnetic field B , we compute the long time limit of the

survival probability $P_s(1)$ in the $E_2;0$ Landau level in two cases. In case (a), the initial state is in the center of the alloy broadened $E_2;0$ 0_{LO} LL's. In case (b), the quantity $P_s(1)$ is computed for every state of $E_2;0$ 0_{LO} and its average $\langle P_s(1) \rangle$ over all these initial states is computed. Then another realization of the disorder is created and both $P_s(1)$ and $\langle P_s(1) \rangle$ are calculated again. Fig. 9 shows the curves $P_s(1)$ and $\langle P_s(1) \rangle$ versus B . If alloy scattering and electron-LO-phonon interactions are the dominant non-radiative losses, the curves shown in Figs. 9(a) and 9(b) can be compared to the output power of the QCL. It appears that the calculated widths are comparable to those seen experimentally [10, 11].

V. CONCLUSION

We have presented a theoretical analysis of the electron-LO-phonon interaction in QCL's structures in the presence of a strong magnetic field and of static short ranged scatterers. Our objective was to ascertain the accuracy of the weak coupling regime between electrons and LO phonons. Our results show that the very notion of a Fermi's golden rule is highly questionable in these structures because of the LL singular density of states. Neither the static scatterers are weak enough nor the electrons and LO phonons form stable magneto-polarons. As a result the survival probability in the upper state of the lasing transition never decays exponentially to zero but displays a number of damped oscillations before stabilizing to $1/2$, thereby evidencing that the magneto-polaron levels never completely empty. Or, the static scatterers are efficient enough to wash out the polaron oscillations because it couples these polaron levels more efficiently to the huge reservoir of uncoupled one-LO-phonon states than to the polaron states. The survival probability in the upper state of the lasing transition decay to zero but not at all in an exponential fashion as would result from the Fermi's golden rule. Instead, it first decays like in the damped polaron case and once has reached its first minimum practically never recovers. The complicated time evolution of the survival probability evidences the need of a more microscopic description to understand the physics of the non-radiative mechanisms in QCL's. It also warns against the estimated efficiency of the static scatterers or phonon scattering when it is based on oversimplified descriptions of the disorder on the QCL quantum states.

Acknowledgments

One of us (Y.C.) would like to thank the French ministry of foreign affairs for financial support. Chen and Zhu would like to also thank the supports from the NSFC (Grant No.10774086), and the Basic Research Program of China (Grant 2006CB921500).

-
- [1] R. F. Kazarinov and R. A. Suris, *Fizika i Tekhnika Poluprovodnikov* 5(4), 797-800 (1971).
- [2] J. Faist, F. Capasso, D. L. Sivco, C. Sirtori, A. L. Hutchinson, and A. Y. Cho, *Science* 264, 553-556 (1994).
- [3] B. S. Williams, *Nature Photon.* 1, 517-525 (2007).
- [4] J. Ulrich, R. Zobl, K. Unterrainer, G. Strasser, and E. Gornik, *Appl. Phys. Lett.* 76, 19 (2000).
- [5] S. Blaser, M. Rochat, M. Beck, D. Hofstetter, and J. Faist, *Appl. Phys. Lett.* 81, 67 (2002).
- [6] C. Becker, C. Sirtori, O. D. Rachenko, V. Rylkov, D. Smirnov, and J. Leotin, *Appl. Phys. Lett.* 81, 2941 (2002).
- [7] D. Smirnov, C. Becker, O. D. Rachenko, V. V. Rylkov, H. Page, J. Leotin, and C. Sirtori, *Phys. Rev. B* 66, 121305 (2002).
- [8] G. Scalari, S. Blaser, J. Faist, H. Beere, E. Linfield, D. Ritchie, and G. Davies, *Phys. Rev. Lett.* 93, 237403 (2004).
- [9] N. Pere-Lapeme, L. A. deVaulchier, Y. Guldner, G. Bastard, G. Scalari, M. Giovannini, J. Faist, A. Vasanelli, S. Dhillon and C. Sirtori, *Appl. Phys. Lett.* 91, 062102 (2007).
- [10] A. Vasanelli, A. Leuliet, C. Sirtori, A. Wade, G. Fedorov, D. Smirnov, G. Bastard, B. Vinter, M. Giovannini and J. Faist, *Appl. Phys. Lett.* 89, 172120 (2006).
- [11] A. Leuliet, A. Vasanelli, A. Wade, G. Fedorov, D. Smirnov, G. Bastard, and C. Sirtori, *Phys. Rev. B* 73, 085311 (2006).
- [12] I. Savic, N. Vukmirovic, Z. Ikonic, D. Indjin, R. W. Kelsall, P. Harrison, and V. Milanovic, *Phys. Rev. B* 76, 165310 (2007).
- [13] V. M. Fomin, V. N. Gladilin, J. T. Devreese, E. P. Pokatilov, S. N. Balaban and S. N. Klimin, *Phys. Rev. B* 57, 2415 (1998).
- [14] T. G. Range, R. Ferreira, and G. Bastard, *Phys. Rev. B* 76, 241304(R) (2007).
- [15] N. Regnault, R. Ferreira and G. Bastard, *Phys. Rev. B* 76, 165121 (2007).
- [16] G. Bastard, *Appl. Phys. Lett.* 43, 591 (1983).
- [17] G. Bastard, *Wave mechanics applied to semiconductor heterostructures*, Wiley-Interscience (1991).
- [18] K. J. Nash, M. S. Skolnick and S. J. Bass, *Semicond. Sci. Technol.* 2, 329-336 (1987).
- [19] C. Becker, A. Vasanelli, C. Sirtori and G. Bastard, *Phys. Rev. B* 69, 115328 (2004).
- [20] C. Cohen-Tannoudji, J. Dupont-Roc, and G. Grynberg, *Photons and atoms : introduction to quantum electrodynamics*, Wiley, New York (1989).
- [21] T. Ando, A. B. Fowler and F. Stern, *Rev. Mod. Phys.* 54, 437 (1982).
- [22] E. A. Zibik, L. R. Wilson, R. P. Green, G. Bastard, R. Ferreira, P. J. Phillips, D. A. Carder, J-P. R. Wells, J. W. Cockburn, M. S. Skolnick, M. J. Steer, and M. Hopkinson, *Phys. Rev. B* 70, 161305(R) (2004).